Electronic Supplementary Information (ESI) for Journal of Materials Chemistry A.
This journal is © The Royal Society of Chemistry 2022

Electronic Supplementary Information

Beyond Hydrophobicity: How F4-TCNQ Doping of the Hole Transport Material Improves Stability of Mesoporous Triple-Cation Perovskite Solar Cells

Maning Liu,[a] Staffan Dahlström,[b] Christian Ahläng,[b] Sebastian Wilken,[b] Aleksandr Degterev,[a] Anastasia Matuhina,[a] Mahboubeh Hadadian,[c] Magnus Markkanen,[d] Kerttu Aitola,[d] Aleksi Kamppinen,[e] Jan Deska,[f] Oliver Mangs,[b] Mathias Nyman,[b] Peter D. Lund,[d] Jan-Henrik Smått,[c] Ronald Österbacka,*[b] Paola Vivo*[a]

[a]Hybrid Solar Cells, Faculty of Engineering and Natural Sciences, Tampere University, P.O. Box 541, FI-33014 Tampere, Finland

[b]Physics, Faculty of Science and Engineering, Åbo Akademi University, 20500 Turku, Finland

[c]Laboratory of Molecular Science and Engineering, Faculty of Science and Engineering, Åbo Akademi University, 20500 Turku, Finland

[d]New Energy Technologies Group, Department of Applied Physics, Aalto University and School of Science, P.O. Box 15100, 00076 Aalto (Espoo), Finland

[e]Faculty of Science and Engineering, University of Turku, FI-20014 Turku, Finland

[f]Department of Chemistry and Materials Science, Aalto University, Espoo, Finland

*Corresponding author.
E-mail: paola.vivo@tuni.fi (P. Vivo); ronald.osterbacka@abo.fi (R. Österbacka)

Table of Contents

1. Experimental details

1.1 Materials

FTO glass substrates (Greatcell Solar, TEC 15), 2 cm × 2 cm, were wet chemically etched with 2M HCl aqueous solution and zinc powder. The etched FTO substrates were then sonicated using an aqueous solution of Hellmanex III solution (2%), acetone and 2-propanol for 15 min in each step, successively. The substrates were then treated with UV-ozone for 15 min to remove organic residuals and increase hydrophilicity. A 30 nm thick compact TiO_2 layer (c-TiO_2) was deposited on the as-prepared patterned substrate by spray pyrolysis of 0.38 M titanium di-isopropoxide bis(acetylacetonate) solution in 2-propanol at 450 °C.[1] The films were then sintered at 450 °C for 1 h in air. The films were cooled down to 150 °C and directly transferred to a dry nitrogen glovebox. A ~200 nm thick active layer of perovskite nanocrystals (NCs) was then deposited on as-prepared c-TiO_2 layers by spin-coating a perovskite NCs solution (100 mg/mL in toluene) at 1500 rpm for 30 s. The perovskite NCs layer was then annealed at 100 °C for 20 min. After annealing, a spiro-OMeTAD layer was spin-coated at 1800 rpm for 30 s. The spiro-OMeTAD solution was prepared by adding 36.2 mg spiro-OMeTAD to 1 ml chlorobenzene and 14.4 µl 4-tBP were stirred using a vortex mixer. Then 8.7 µl Li-TFSI solution and 14.5 µl FK209 pre-dissolved in acetonitrile were added to the spiro-OMeTAD solution with concentrations of 520 mg/ml and 300 mg/ml, respectively. Finally, an 80 nm thick gold contact was thermally evaporated on top of the spiro-OMeTAD layer to form the back contact. Evaporation was conducted in high vacuum (6×10^{-6} mbar).

1.2 Device fabrication and film preparation

CsFAMA-based perovskite solar cells were fabricated with a reported one-step method.[1] In a typical fabrication process, FTO glass substrates (2 cm × 2 cm) were wet chemically etched with 2M HCl aqueous solution and zinc powder. The etched FTO substrates were then sonicated using an aqueous solution of Mucasol solution (2% in water), acetone and 2-propanol for 15

min in each step, successively. After swiftly drying with compressed dry air (CDA), the substrates were treated with UV-ozone for 15 min to remove organic residuals and increase hydrophilicity. A ~30 nm thick (determined by a surface profiler, Dektak 150 stylus profilometer) compact TiO_2 layer (c-TiO_2) was deposited on the as-prepared FTO substrate by spray pyrolysis of 0.38 M TDBA solution in 2-propanol at 450 °C. The films were then sintered at 450 °C for 1 h in air. A mesoporous TiO_2 (m-TiO_2) scaffold layer was made by spin coating an ethanolic suspension of 30NRD TiO_2 nanoparticle paste (150 mg TiO_2 paste in 1 mL ethanol) at 4000 rpm for 10 s. The films were quickly dried at 100 °C for 10 min prior to calcination at 450 °C for 30 min under a continuous air flow. The films were then cooled down to 150 °C and directly transferred into a nitrogen-filled glovebox. To make a ~500 nm thick CsFAMA perovskite film, the perovskite precursor was first prepared comprising FAI (0.95 M), PbI_2 (1.1 M), MABr (0.19 M), $PbBr_2$ (0.2 M), and CsI (0.06 M) in a mixed solvent of DMF:DMSO (4:1, v:v). 50 µl solution was spin-coated onto the as-prepared FTO/c-TiO_2/m-TiO_2 substrate at 1000 rpm for 10 s, followed by 6000 rpm for 20 s. 100 µl chlorobenzene were swiftly dropped as the anti-solvent treatment 5 s prior to the programming end. The perovskite layer was then annealed at 110 °C for 1 h. The resulting perovskite composition comprises a stoichiometry of $Cs_{0.05}(FA_{0.83}MA_{0.17})_{0.95}Pb(I_{0.83}Br_{0.17})_3$, namely CsFAMA perovskite.[2] After annealing, the different concentrations (1–6%, mol%) of F4-TCNQ doped spiro-OMeTAD layer, or the reference doped Spiro-OMeTAD layer was dynamically spin-coated at 1800 rpm for 40 s on top of as-formed perovskite layer. The reference doped Spiro-OMeTAD solution was obtained by first adding 36.2 mg Spiro-OMeTAD and 14.4 µl 4-tBP to 1 ml chlorobenzene, which was stirred at 60 ℃ for 3 min. Then 8.7 µl Li-TFSI (520 mg/mL) and 14.5 µl FK209 (300 mg/mL) pre-dissolved in acetonitrile were added to the spiro-OMeTAD solution, respectively. Finally, a 100 nm thick gold electrode was thermally evaporated in a vacuum of 5×10^{-4} mbar on top of the HTM layer.

Roughly 100 nm thick spiro-OMeTAD films for four-point probe conductivity measurements were spin-coated on square sized PET-substrates 2.5 cm × 2.5 cm. The films were doped by tBP:LiTFSI:FK209 (same protocol as described in the solar cell fabrication above) or 2 mol% F4-TCNQ.

1.3 Simulation method

The drift-diffusion simulations were performed with a previously published model.[3,4] The code used to run the simulations can be found at https://github.com/cahlang/2DDriftDif and the details of the simulation framework in Ref [3]. We performed one-dimensional simulations, including both charge transport layers and the perovskite layer. We assumed a uniform generation rate in the perovskite layer, with the generation rate estimated from the measured J_{SC} of the reference samples. We took the recombination in the perovskite layer to be a combination of direct and trap-assisted recombination, with the trap-assisted recombination lifetime determined from the TRPL data. We assumed that the recombination rate at the CTL/perovskite interfaces is purely trap-assisted with a shorter lifetime compared to the bulk process. We estimated the transfer velocity across the perovskite/Spiro interface from the TRPL data. We based the conductivity of the Spiro layer in the simulation on the data from the conductivity measurements. The other simulation parameters used are typical for perovskite soalr cells (PSCs)[3] and the (qualitative) simulation results do not depend strongly on the exact value of these. The full list of simulation parameters is presented in **Table S3**.

1.4 Characterization

Ultraviolet and visible absorption (UV−vis) spectra were recorded with a dual-beam grating Shimadzu UV-1800 absorption spectrometer. Photoluminescence (PL) spectra were measured with a FLS1000 spectrofluorometer (Edinburgh Instruments, UK). The time-resolved PL (TRPL) decays were obtained by using a time-correlated single photon counting (TCSPC)

apparatus equipped with a Picoharp 300 controller and a PDL 800-B driver for excitation and a Hamamatsu R3809U-50 microchannel plate photomultiplier for detection in 90° configuration. The instrument response time was 60 ps.

The cross-section image of the device was obtained using a field emission scanning electron microscope (FESEM, LEO-1530 Gemini, Germany) at 36.24 kx magnification. Bruker's Nanoscope V MultiMode 8 atomic force microscope (AFM) was used to image the topography of the spiro-OMeTAD samples on glass substrates using the silicon cantilevers with a nominal tip radius 10 nm (NSG10, NT-MDT, Russia). The AFM images of the thin film samples were obtained in tapping mode at ambient atmosphere. Images (2 μm × 2 μm) with a resolution of 1024 by 1024 pixels were captured at a scan speed of ca. 1 line per second. The image analysis and calculation of the surface roughness values were conducted by Scanning Probe Image Processor (SPIP) by Image Metrology (Denmark).

Conductivity measurements were performed under nitrogen atmosphere using a four-point probe setup in a linear configuration with spring-loaded gold probes with a spacing of 1.79 mm. A source meter (Keithley 2400) was used for applying a current on the outer probes, while the voltage decay over the inner probes was measured. The measured voltage as a function of current showed a linear behavior in the measured regime. Conductivities were calculated using finite-size corrections.[5] Each measurement was carried out on two different positions on the square sized films by turning the sample 90 degrees. Water contact angle (CA) measurements were conducted by using Attension Theta Lite optical goniometer (Biolin Scientific AB, Sweden).

The unencapsulated perovskite solar cells were characterized under ambient conditions (RH~40%, RT = 23 ± 1°C). The active area of each cell was determined by the size of the aperture (20 mm^2), and precisely assessed by an optical Dino-Lite AM4113ZTL microscope. The current density (*J*)-voltage (*V*) characteristics were recorded with a Keithley 2450 source-monitor unit, under air mass (AM) 1.5 simulated sunlight (100 mW/cm^2). The 1 sun

illumination was generated through an AAA- solar simulator (Sciencetech Inc), which was calibrated with a silicon reference cell. The bias scan rate was 20 mV/s and a preconditioning time of 5 s was applied. For the stability study, all tested cells were stored under ambient conditions (in dark, RH~40%).

For long-term stability measurement with maximum power point tracking, the PSCs were aged under a large area white LED lamp and in their maximum power points (MPP). Since the MPPs of PSCs are likely to change during the aging, the MPP measurements need to be performed repeatedly (MPP tracking, MPPT) and the cells kept at their MPPs with programmable resistors between the MPP measurements. The MPPT for the PSCs was performed with an in-house built solar cell aging testing unit (SCATU) developed originally for dye solar cell aging measurements, modified by adding automated, periodical MPPT measurements and possibility to keep solar cells at their MPPs with programmable resistors, between the periodical *J–V* and MPPT measurements, to it.[6] In the MPPT, SCATU first performs a *J–V* measurement and determines an estimate for the maximum power point voltage (V_{mpp}). Using this estimate as the V_{mpp}, SCATU measures voltages in certain intervals around the estimate. The user specifies the size of these intervals, and SCATU measures five intervals above and below the estimated $V_{mpp.}$ If the measured V_{mpp} is close enough to the estimate, SCATU accepts the measured voltage as the V_{mpp} and uses the value in choosing the resistor (load) which to apply to the individual cell to keep it at its MPP. Since the voltage is measured in set intervals or steps, the acceptance range around the estimated V_{mpp} must be determined by these intervals. In these measurements the voltage intervals were chosen to be 10 mV and the acceptance range was 20 mV. If the V_{mpp} is not within the acceptance range, SCATU performs the MPPT again using the newly found V_{mpp} as the new estimate. This procedure is repeated until the V_{mpp} obtained from the MPPT is close enough to the estimate or until the MPPT has been carried out 11 times. After 11 trials, SCATU accepts the newest measured V_{mpp} as the accurate voltage even if it is not very close to the estimate. The 11 trials limit is set as a safety measure, in order to keep the measurement

running, in case the MPPT would end up in an indefinite loop, while e.g. measuring a very hysteretic and/or a very degraded PSC.

2. Results

2.1 Additional experimental data

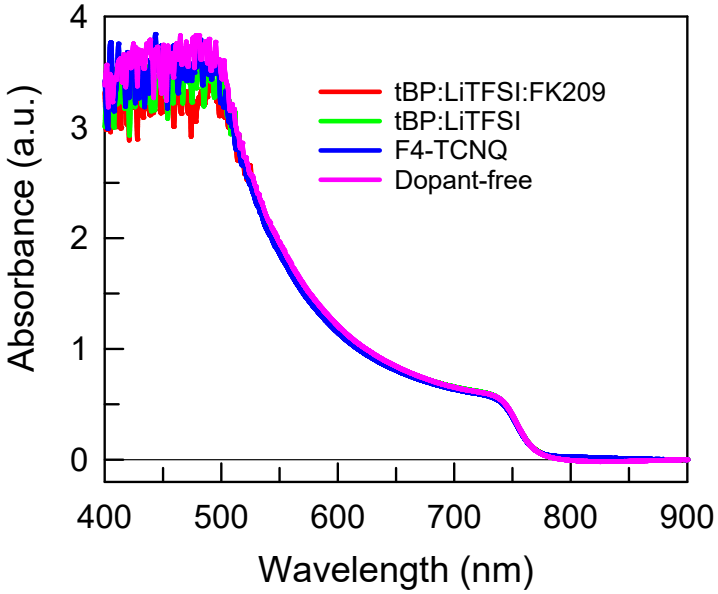

Figure S1. Absorption spectra of glass/perovskite/spiro-OMeTAD samples, where spiro-OMeTAD is doped with various additive combinations.

Table S1. Performance of champion perovskite solar cells where spiro-OMeTAD is doped with F4-TCNQ at different concentrations (mol%). All data are obtained from the reverse scan.

mol%	PCE (%)	J_{sc} (mA cm^{-2})	V_{oc} (V)	FF (%)
1.0 %	13.3	21.9	1.03	59.1
1.5 %	14.3	21.6	1.08	61.6
2.0 % (optimized)	14.6	20.7	1.09	64.8
3.0 %	13.0	21.3	1.04	58.6
4.0 %	12.6	20.6	1.04	59.1
6.0 %	12.0	20.4	1.00	58.9

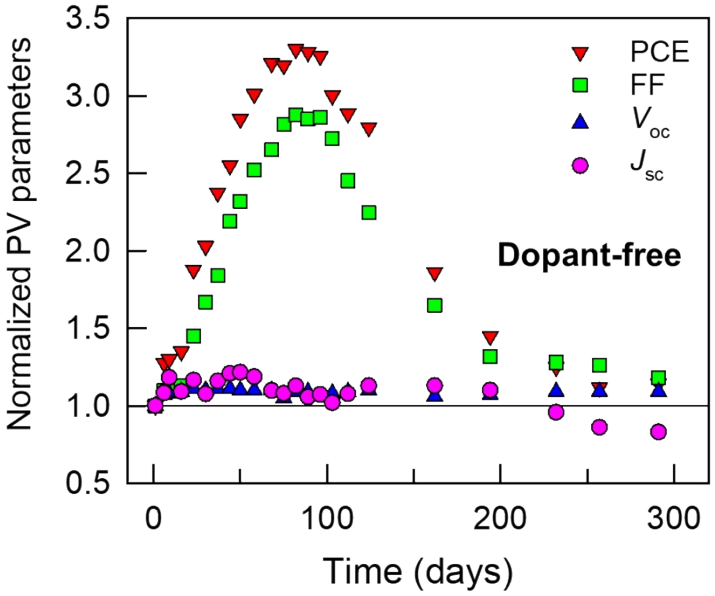

Figure S2. Normalized photovoltaic parameters of the best device with no doped spiro-OMeTAD vs. storage time, stored in air (darkness, RH~40%).

Table S2. Summary of WCAs for differently doped spiro-OMeTAD films coated on perovskite films.

Dopants	CA left (°)	CA right (°)	CA mean (°)
tBP & LiTFSI & FK209	65.9	65.6	65.8
tBP & LiTFSI	77.9	76.1	77.0
F4-TCNQ	86.2	86.8	86.5

2.2 PSC aging with maximum power point tracking

An estimate of the MPP was first determined with an automatically conducted *J–V* measurement, and a more accurate MPP was found with MPPT using the estimated MPP, obtained from the *J–V* measurement, as the initial value for the tracking algorithm. The *J–V* and MPPT measurements were repeated periodically during the aging measurement, and between those measurements, the cells were kept at their MPPs with programmable loads. The aging measurements were performed with CsFAMA PSCs with three differently doped spiro-OMeTAD layers, i.e., dopant-free, reference doped (tBP:LiTFSI:FK209), and F4-TCNQ doped spiro-OMeTAD. The cells were left unencapsulated in the aging measurements, which was consistent with the shelf-storage conditions. The long-term stability measurements were conducted with 18 cells in total (i.e., six cells for each type of doped spiro-OMeTAD). The long-term evolution of the photovoltaic parameters of the cells, obtained automatically with

periodical J–V measurements with SCATU, are shown in **Figure S3**. The results of the MPPT obtained with SCATU are shown in **Figure S4**. By comparing Figure S3a with Figure S4, we can conclude that the evolution of the PCE, obtained from the periodical J–V measurements, resembles closely that of the P_{MPP} (the power at maximum power point), obtained from the MPPT measurements. It is noted that on average the F4-TCNQ doped cells were more stable particularly in the change of FF, i.e., degraded slower than the reference doped cells since the relatively fast degradation for all types of doped cells was expected in the case of unencapsulated PSCs aged under ambient conditions.[7] For the dopant-free and F4-TCNQ doped cells, the V_{oc} first decreased and then increased during the aging measurement, finally surpassing the V_{oc} of the standard doped cells. The better long-term stability of the F4-TCNQ doped cells compared to that of the reference cells is in line well with the results from the studies on the shelf-storage stability.

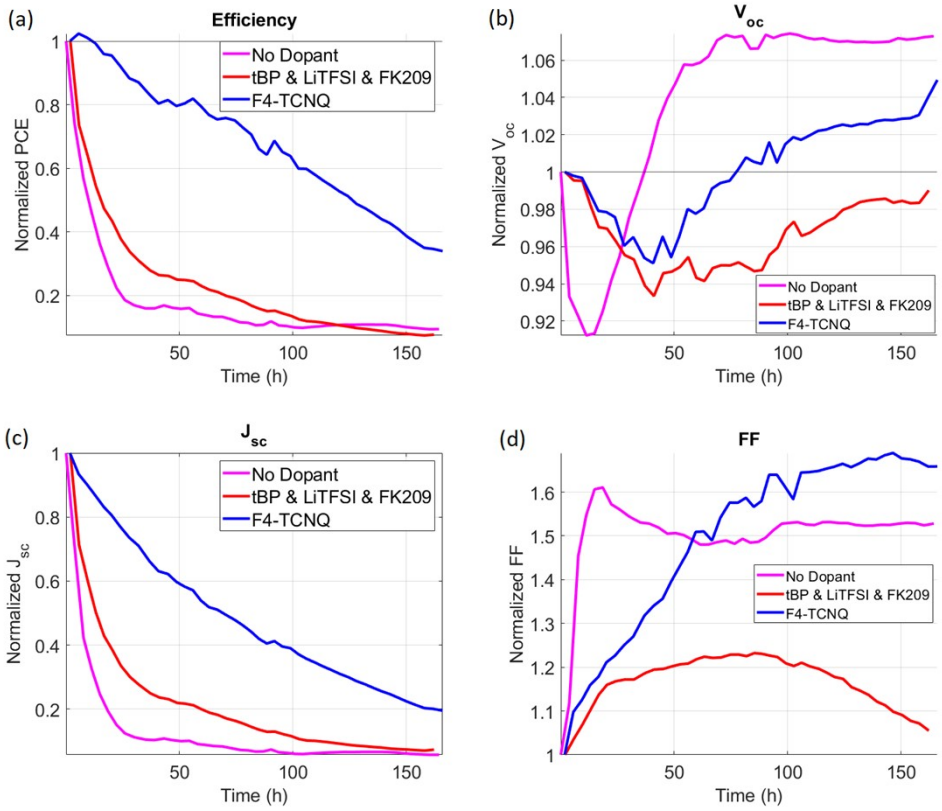

Figure S3. Evolution of the photovoltaic parameters in the long-term stability measurement, obtained from periodical J–V measurements.

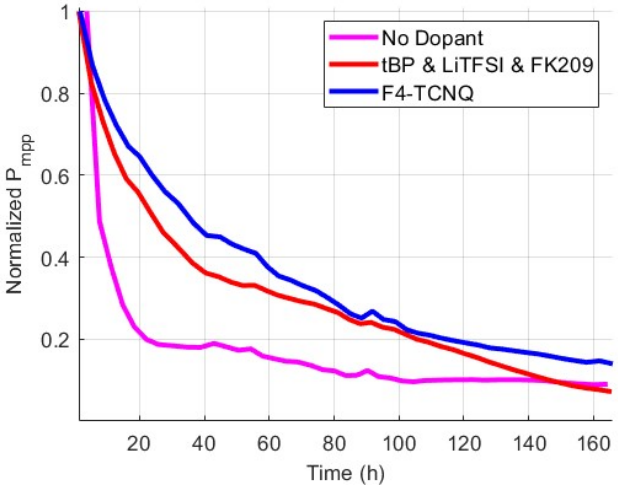

Figure S4. Evolution of the maximum power point of the cells in the aging measurement, obtained with the maximum power point tracking.

2.3 Thermal stability test

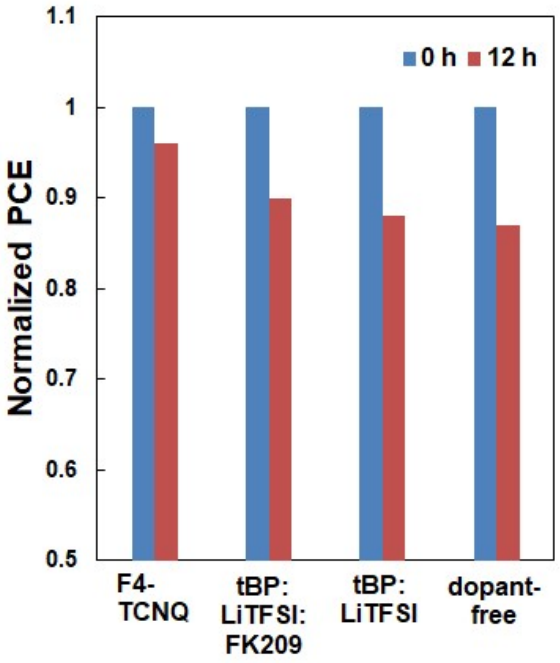

Figure S5. Normalized PCEs of PSCs employing different dopants in the spiro-OMeTAD layer as a function of thermal heating time (at 65 °C in nitrogen atmosphere).

2.4 Storage-time dependent TRPL decays

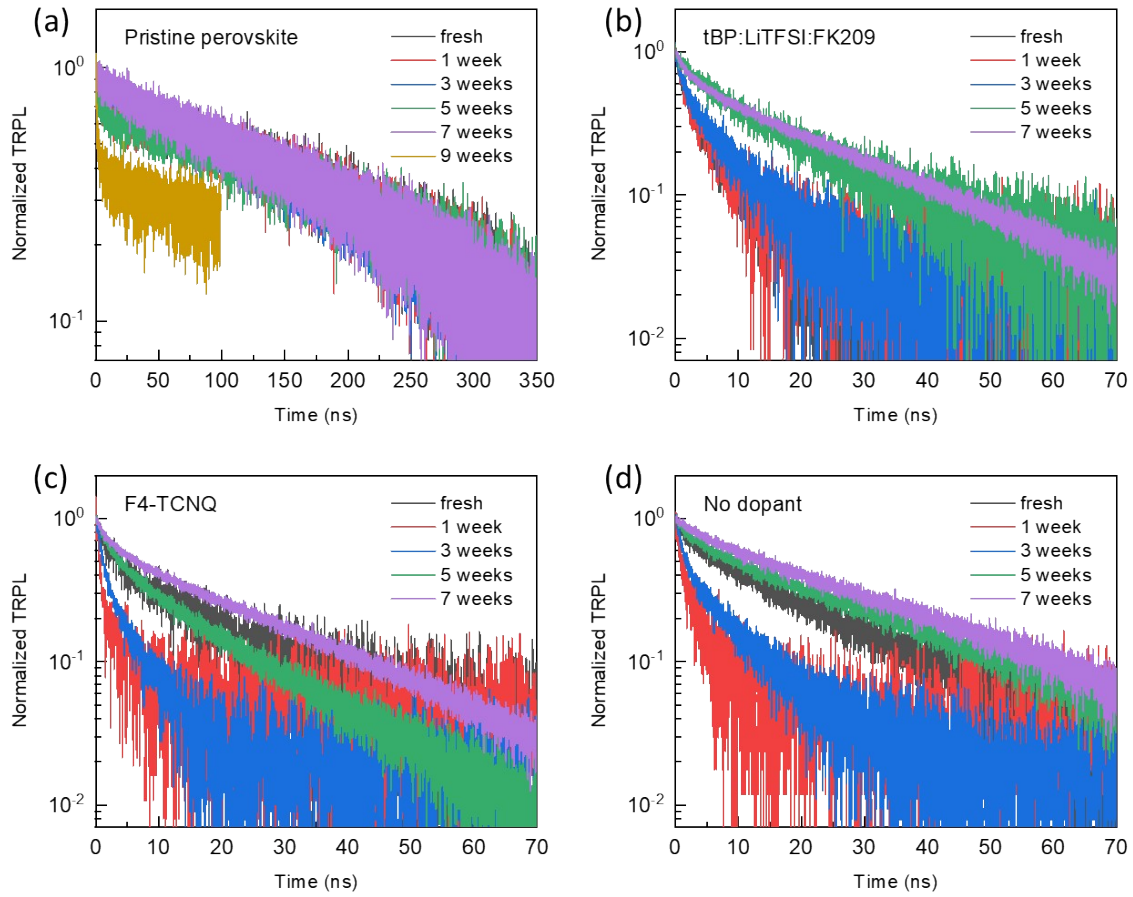

Figure S6. Storage time dependent TRPL decays of (a) glass/perovskite and (b-d) glass/perovskite/spiro-OMeTAD with different dopant combinations, excited at 483 nm, and monitored at 765 nm. All films are stored in air (darkness, RH~40%).

2.5 Drift-diffusion simulations

Table S3. Material and layer properties used in the drift-diffusion simulations.

Parameter	**Perovskite**	**spiro-OMeTAD**	**ETM**
Thickness (nm)	400	120	200
Valence band (eV)	5.4	5.35	7
Conduction band (eV)	3.8	3.5	3.8
Hole mobility ($cm^2\ V^{-1}s^{-1}$)	20	10^{-4}	
Electron mobility ($cm^2\ V^{-1}s^{-1}$)	20		2×10^{-3}
Relative dielectric constant	30	3	10
Generation Rate ($cm^{-3}\ s^{-1}$)	3.5×10^{27}		

Direct recombination coefficient ($cm^3\ s^{-1}$)	5×10^{-19}		
Trap-assisted recombination lifetime (ns)	450		
Perovskite/CTL interface recombination lifetime (ns)		100	10^4
Perovskite/CTL transfer velocity ($cm\ s^{-1}$)		2700	100
Contact injection barrier (eV)		0.15	0.1

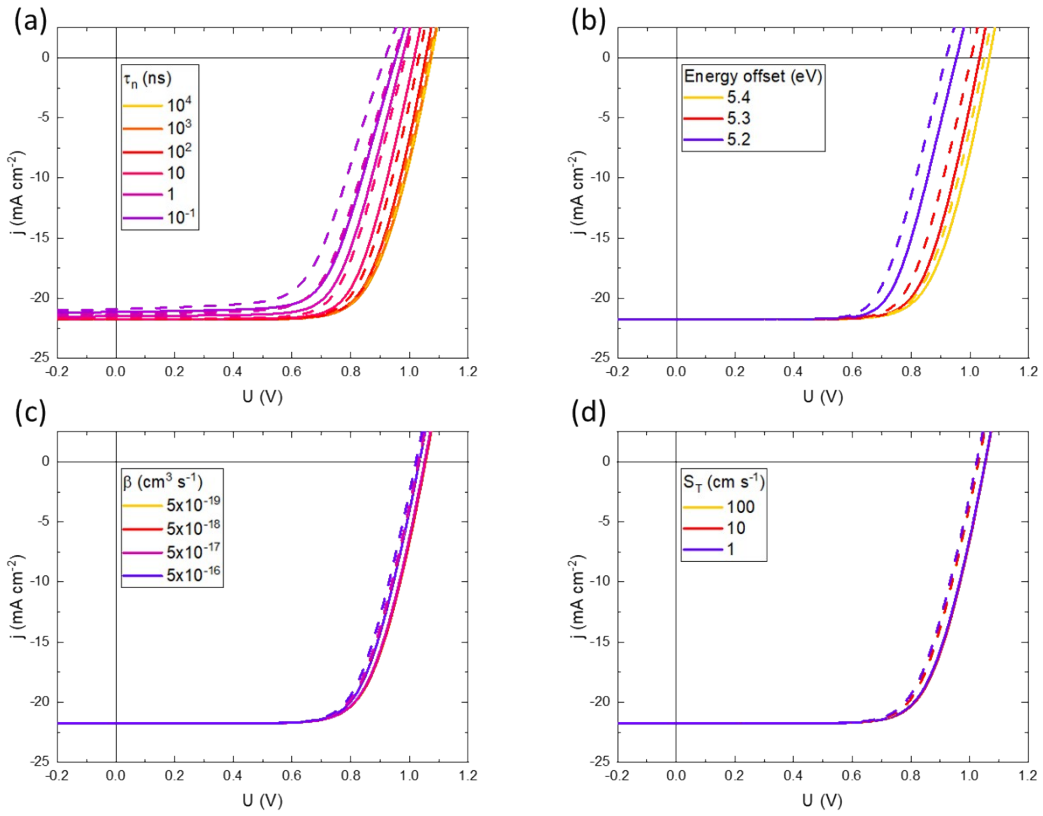

Figure S7. Simulation data for varying (a) interface recombination lifetime τ_n at the spiro/perovskite interface, (b) energy offset, (c) direct recombination coefficient β, and (d) transfer velocity S_T across the perovskite/spiro-OMeTAD interface.

2.6 Stability study on the devices stored in a dry cabinet (RH<10%)

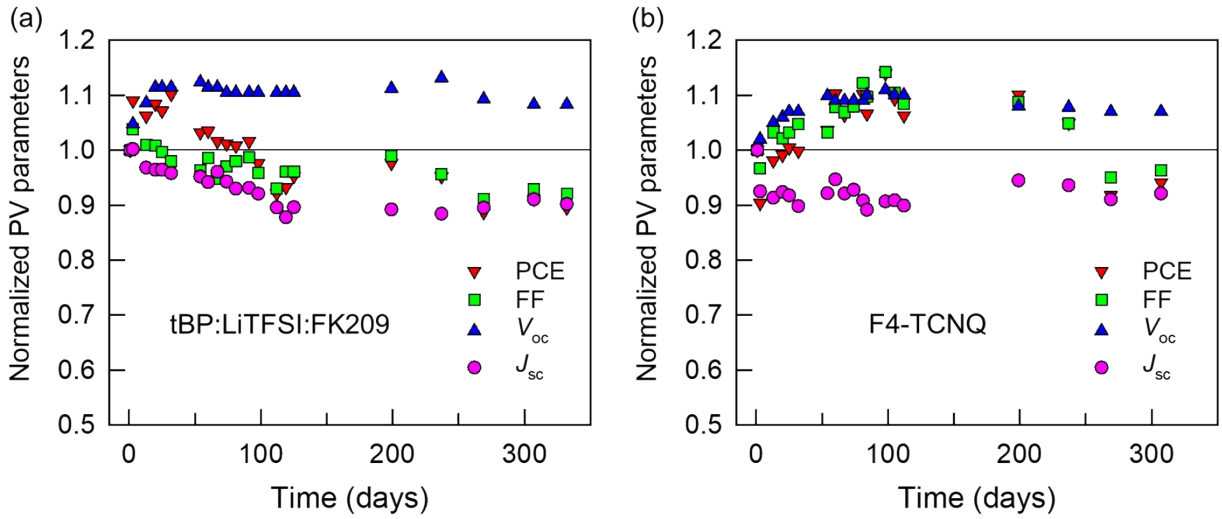

Figure S8. Normalized photovoltaic parameters of the best devices with (a) reference doped and (b) F4-TCNQ doped spiro-OMeTAD vs. storage time, stored in a dry cabinet (darkness, RH<10%).

References

1 H. Zhang, M. Liu, W. Yang, L. Judin, T. I. Hukka, A. Priimagi, Z. Deng and P. Vivo, *Adv. Mater. Interfaces*, 2019, **6**, 1–10.

2 M. Saliba, J.-P. Correa-Baena, C. M. Wolff, M. Stolterfoht, N. Phung, S. Albrecht, D. Neher and A. Abate, *Chem. Mater.*, 2018, **30**, 4193–4201.

3 C. Ahläng, M. Nyman and R. Österbacka, *Phys. Rev. Appl.*, 2021, **16**, 014041.

4 C. Ding, R. Huang, C. Ahläng, J. Lin, L. Zhang, D. Zhang, Q. Luo, F. Li, R. Österbacka and C. Q. Ma, *J. Mater. Chem. A*, 2021, **9**, 7575–7585.

5 F. M. Smits, *Bell Syst. Tech. J.*, 1958, **37**, 711–718.

6 A. Kamppinen, K. Aitola, A. Poskela, K. Miettunen and P. D. Lund, *Electrochim. Acta*, 2020, **335**, 135652.

7 Y. Guo, H. Lei, L. Xiong, B. Li and G. Fang, *J. Mater. Chem. A*, 2018, **6**, 2157–2165.